nature nanotechnology

ARTICLES

PUBLISHED ONLINE: 20 FEBRUARY 2011 | DOI: 10.1038/NNANO.2011.11

Giant magnetoresistance through a single molecule

Stefan Schmaus[1,2], Alexei Bagrets[2,3], Yasmine Nahas[1,2], Toyo K. Yamada[1,4], Annika Bork[1], Martin Bowen[5], Eric Beaurepaire[5], Ferdinand Evers[3,6] and Wulf Wulfhekel[1,2]*

Magnetoresistance is a change in the resistance of a material system caused by an applied magnetic field. Giant magnetoresistance occurs in structures containing ferromagnetic contacts separated by a metallic non-magnetic spacer, and is now the basis of read heads for hard drives and for new forms of random access memory. Using an insulator (for example, a molecular thin film) rather than a metal as the spacer gives rise to tunnelling magnetoresistance, which typically produces a larger change in resistance for a given magnetic field strength, but also yields higher resistances, which are a disadvantage for real device operation. Here, we demonstrate giant magnetoresistance across a single, non-magnetic hydrogen phthalocyanine molecule contacted by the ferromagnetic tip of a scanning tunnelling microscope. We measure the magnetoresistance to be 60% and the conductance to be $0.26G_0$, where G_0 is the quantum of conductance. Theoretical analysis identifies spin-dependent hybridization of molecular and electrode orbitals as the cause of the large magnetoresistance.

Spin-polarized transport through a single molecule has attracted interest, because it combines the goals of downward size scaling of electronic components (to lower power consumption while increasing speed and density) and increasing computational bandwidth by manipulating spin in addition to charge. The concept of spin electronics[1,2] was pioneered with the discovery that the resistance of two ferromagnetic layers separated by a thin non-magnetic spacer may be driven by an external magnetic field or the flow of charge. In the case of a thin metallic spacer, this effect is termed giant magnetoresistance (GMR)[3,4], and for ultrathin insulating layers it is called tunnelling magnetoresistance (TMR)[5,6]. Across thin organic semiconducting layers, transport may occur via tunneling or sequential tunneling, that is, diffusive hopping[7,8], demonstrating a magnetoresistance thanks to the low values of spin–orbit coupling, despite the presence of defects in these imperfectly mastered semiconductors[9,10].

Spin electronics has led to new generations of read heads in hard disk drives and random access memory, but further progress in downsizing spintronic devices has been challenging. Indeed, although TMR values may dwarf those of their GMR counterparts through a judicious selection of ferromagnets[11] and inorganic[12] or organic[13,14] tunnel barriers, downsizing such devices can lead to high resistances[8] and shot noise, which are incompatible with high-frequency applications[15]. Separately, as the device size is reduced, the GMR bias output shrinks below the bias drop of the leads, which in turn requires one to artificially lower the current densities to achieve a high magnetic sensitivity[16].

A promising approach to extreme downsizing has been to study electronic single-molecule devices such as diodes[17] and transistors[18–20]. Turning now to molecular spintronics, recent studies have described the spintronic impact of chemisorption of molecules[21] onto ferromagnets. This highly conductive interface[22] can drive spintronic properties[8,21], due in part to ferromagnetic coupling between the transition metal site of the molecule and the ferromagnetic surface[21,23,24].

Here, we present a combined experimental and theoretical study on spin-polarized charge transport across a single molecule in the GMR regime that takes advantage of these novel molecular spintronic properties. The junction, built with the help of a scanning tunnelling microscope (STM), consists of two ferromagnetic electrodes bridged by a hydrogen phthalocyanine ($H_2Pc = C_{32}H_{18}N_8$) molecule. Our study shows that, due to charge transfer towards the molecule and the hybridization of molecular orbitals near the Fermi level with bulk electronic states of the electrodes, transport across the molecule is nearly resonant in the minority channel with an ultralow areal resistance product. Surprisingly, the molecule can sustain a large current density with substantial spin-polarization, thus validating the concept of nanoscale spintronic devices. Indeed, despite the absence of transition metal sites on the molecule that could contribute to spin filtering, we observe a high differential GMR value of ~60% across the molecular junction, with an areal resistance product of only 70 $\mu\Omega\,\mu m^2$. Our *ab initio* theoretical analysis explicitly identifies this effect as a strong, generic, spin-dependent hybridization mechanism that can also dominate the magnetoresistance in the TMR regime, as was reported phenomenologically[8].

Sample characterization

STM[25–27] and break-junction[28,29] techniques have generally proven to be powerful and versatile tools with which to study the transport properties of single-molecule junctions. In this work, we use magnetic electrodes to measure the magnetoresistance of single molecules using spin-polarized STM (Sp-STM). Experiments were carried out in a home-built STM instrument working in ultra-high vacuum at 4 K (ref. 30) on individual H_2Pc molecules sandwiched between cobalt-coated tungsten tips and ferromagnetic cobalt nano-islands on Cu(111) single crystals (see Supplementary Information).

Figure 1a presents the STM topography of the sample. The cobalt nano-islands exhibit a spontaneous out-of-plane magnetization due to a strong interfacial anisotropy[31,32]. With cobalt-coated tips

[1]Physikalisches Institut, Karlsruhe Institute of Technology (KIT), 76128 Karlsruhe, Germany, [2]DFG-Center for Functional Nanostructures, Karlsruhe Institute of Technology (KIT), 76128 Karlsruhe, Germany, [3]Institute of Nanotechnology, Karlsruhe Institute of Technology (KIT), 76128 Karlsruhe, Germany, [4]Graduate School of Advanced Integration Science, Chiba University, Chiba 263-8522, Japan, [5]Institut de Physique et Chimie des Matériaux de Strasbourg, UMR 7504 UdS-CNRS, 67034 Strasbourg Cedex 2, France, [6]Institut Für Theorie der Kondensierten Materie, Karlsruhe Institute of Technology (KIT), D-76128 Karlsruhe, Germany. *e-mail: wulf.wulfhekel@kit.edu

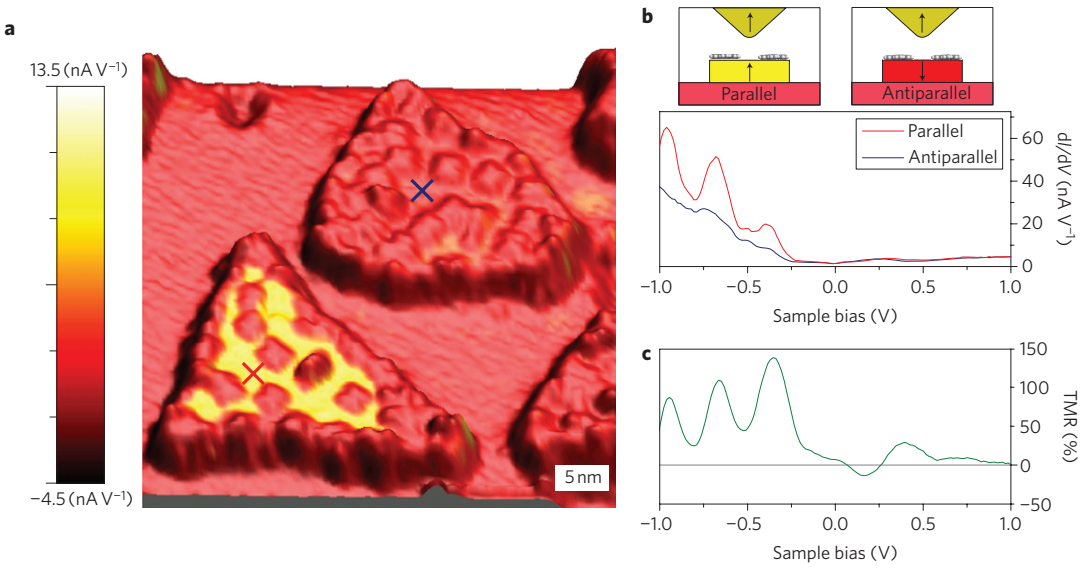

Figure 1 | H_2Pc molecules adsorbed on cobalt islands with different out-of-plane magnetic orientations. a, Topographic image of H_2Pc molecules adsorbed onto two cobalt islands on the Cu(111) surface. Colour code: measured dI/dV at −310 mV. The two island species can be distinguished by the magnetization parallel (in yellow) and antiparallel (in red) to the tip magnetization. **b**, Typical dI/dV spectra taken on parallel and antiparallel oriented cobalt islands (marked by red and blue crosses in **a**) clearly reveal spin-polarized density of states below the Fermi edge. **c**, Energy dependence of the optimistic TMR ratio calculated from the dI/dV spectra. The highest value is measured at approximately −350 meV, and is used to distinguish between the magnetic orientation of the islands.

(10 monolayers) showing an out-of-plane magnetization, we can use the sensitivity of the Sp-STM technique to the spin-polarized density of states[33] to determine the orientation (parallel or antiparallel) of the magnetization of individual islands relative to that of the tip. Figure 1b shows typical differential conductance (dI/dV) curves measured on top of cobalt islands of parallel and antiparallel orientation. Particularly large differences in the spectra are found at −350 meV, which corresponds to the surface state of cobalt[34]. By recording maps of the differential conductance at this bias voltage (Fig. 1a), we can thus identify the spin orientation of the cobalt islands and determine the differential TMR. The latter is defined as the difference in differential conductance (dI/dV) divided by the smaller differential conductance of the tunnel junction formed by the tip and cobalt island for ensembles of junctions with parallel and antiparallel oriented cobalt islands. As can be seen in Fig. 1c, the differential TMR for such cobalt/vacuum/cobalt junctions is strongly energy-dependent, as reported previously[32]. Remarkably, the differential TMR reaches only ∼5% at low bias voltage.

Spin-dependent conductance across a single molecule

The H_2Pc molecules that were also deposited adsorb lying flat on the cobalt surface[24], and are therefore easily recognized in Fig. 1 by their four aromatic isoindole (BzPy) side groups[35]. Although the local spin-polarization in the tunnelling regime has been imaged with Sp-STM for phthalocyanine molecules with 3d metal centres[24,36], we here focus on GMR transport measurements across non-magnetic H_2Pc molecules in the contact regime. To observe the transition from the TMR regime to the GMR regime across the molecule, we alter the junction geometry and achieve tip-to-molecule contact by positioning the STM tip above the aromatic side groups of a H_2Pc molecule, opening the feedback loop and decreasing the tip-to-molecule distance by a small offset (∼1 Å s^{-1}) while measuring the tunnelling current[25–27,37,38]. We first observe an exponential increase of the conductance due to the decreasing tunnelling barrier width (Fig. 2a). Below a certain tip-to-surface separation (typically 3–4 Å), the conductance abruptly increases and thereafter depends only weakly on the distance. As reported regarding alkanedithiol molecular wires[26], this underscores the 'jump-to-contact' of a molecular segment. For H_2Pc molecules, the transition between the flat adsorption and the contact geometry has been ascribed to the 20 meV vibrational bending mode of the aromatic side groups of the H_2Pc molecule. Note that when voltages higher than this vibrational mode are applied in the contact geometry, the vibration can be excited by the current and the molecular contact becomes unstable (see Supplementary Information).

The conductance after the jump-to-contact encompasses two contributions: the current across the molecule G_{mol} and a leakage current G_{tun} due to direct tunnelling between the tip and sample[26] (Fig. 2c). To obtain a reasonable estimate of the molecular conductance G_{mol}, we therefore subtract the conductance G_{tun} measured before the jump from the conductance G_{cont} measured after the jump, that is, $G_{mol} \approx G_{cont} - G_{tun}$. Because measurements on two parallel and antiparallel oriented cobalt islands are required, using identical tip conditions, to extract the GMR correctly, we record the traces from two such islands in the same topographic scan. This method notably eliminates possible magnetostriction effects between the two ferromagnetic electrodes, because neither the tip nor the island magnetization need be switched by an external magnetic field.

In the particular measurement at 10 mV in Fig. 2a, we find a conductance of $G_P = 0.26G_0$ for the parallel and $G_{AP} = 0.19G_0$ for the antiparallel magnetic configuration in units of $G_0 = 2e^2/h$. These rather large conductance values underscore a strong hybridization between the electronic levels of the metallic electrodes and those of the molecule[21]. This is in sharp contrast to the orders of magnitude lower values reported for almost insulating molecular TMR devices[8,13] and single-molecule devices based on C_{60} (ref. 39).

Each such measurement was repeated several hundred times on the four side groups of about 10 molecules adsorbed onto the two parallel and antiparallel oriented islands, leading to a distribution of the conductances across these parallel-type and antiparallel-type junctions as depicted in Fig. 2d. Compared to previous results[26], the width of the resulting conductance distribution is relatively narrow. The broadening and possible structural elements of these distributions could reflect variation in the contact and binding geometries, but also fluctuations in the spin-polarized density of states

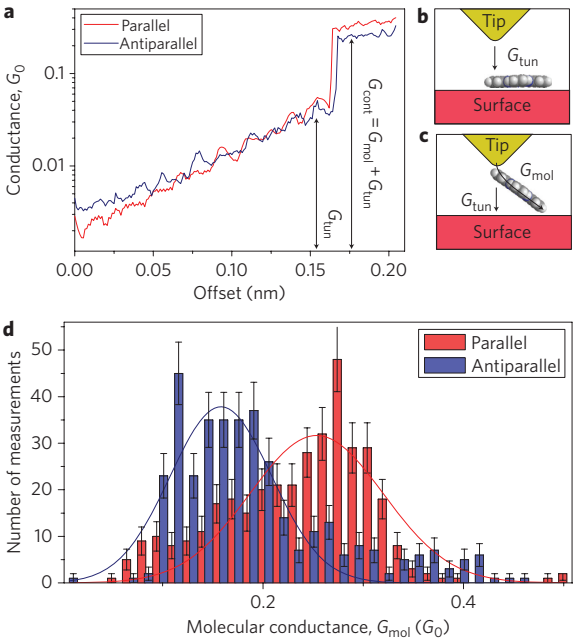

Figure 2 | Current–distance traces and magnetoresistance measured across single H_2Pc molecules. a, Typical set of conductance-distance curves measured on top of a H_2Pc molecule adsorbed onto parallel and antiparallel magnetized islands with a constant tunnelling voltage of 10 mV ($G_0 = (2e^2/h)$). **b**, As the tip approaches the molecule, the tunnel barrier width decreases, so the conductance increases exponentially. **c**, Below a certain tip-to-surface separation (typically 3–4 Å) the conductance abruptly increases as the molecule jumps into contact, and then varies only slightly upon further reducing the distance. Transport across the contacted molecule reflects both tip-to-surface tunnelling and conduction across the molecule. **d**, Histogram of corrected molecular conductances (381 parallel and 366 antiparallel). A Gaussian fit is used to determine the statistical conductance in the parallel and antiparallel configurations, and thus the GMR ratio. Error bars indicate statistical errors in the conductance distribution.

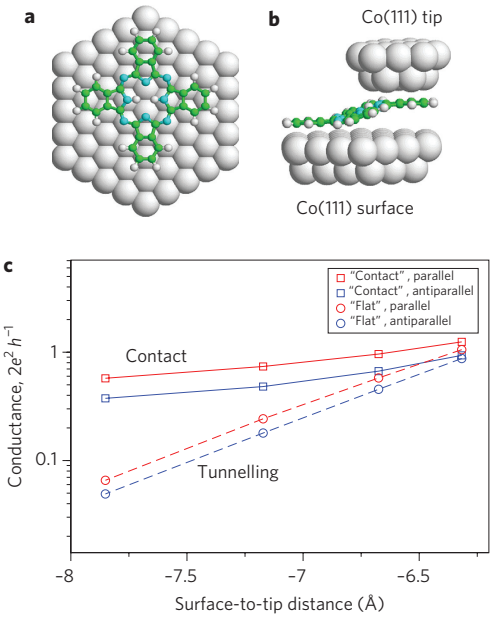

Figure 3 | *Ab initio* simulations of current–distance traces and the magnetoresistance effect across a H_2Pc molecule. a,**b**, Contact geometry used in the transport calculation: for a H_2Pc molecule adsorbed on the Cobalt island (**a**), and in simultaneous contact with the tip and the cobalt surface through a lifting of the aromatic group (**b**). Cobalt sites, grey; hydrogen, white; carbon, green; nitrogen, cyan. **c**, Conductance of H_2Pc sandwiched between two parallel or antiparallel aligned Co(111) surfaces in the tunnelling (before contact) and ballistic (after contact) junction geometries.

on the islands[32,40]. Gaussian fits were used to determine the average conductances and the GMR from the measurement statistics. We find $G_P = (0.253 \pm 0.005)G_0$ and $G_{AP} = (0.158 \pm 0.005)G_0$. These values result in an optimistic GMR ratio at $V = 10$ mV of

$$\mathrm{GMR} = \frac{G_P - G_{AP}}{G_{AP}} = (61 \pm 9)\%$$

Surprisingly, this GMR ratio is one order of magnitude larger than the differential TMR ratio found for direct tunnelling between the tip and the cobalt surface.

Transport calculations

To understand what causes this large value of GMR, we performed transport calculations based on density functional theory (DFT) using the non-equilibrium Green's function (NEGF) formalism and the TURBOMOLE package[41] (see Supplementary Information). The atomic structure of the molecular junction was found by optimizing the H_2Pc geometry on a Co(111) surface that was modelled using a 65-atom cluster. Our analysis suggests that H_2Pc adsorbs preferentially in the bridge position onto Co(111) (Fig. 3a), due to a binding energy −8.17 eV that is larger than the one found in either the hollow site position (−8.06 eV) or the atop site position (−7.45 eV), which is consistent with earlier findings[24,42].

We have calculated spin-polarized transport in the linear response at low bias voltage for two junction geometries, schematically shown in Fig. 3a,b, corresponding to the TMR and GMR transport regimes (see Supplementary Information). Qualitatively, these calculations (Fig. 3c) reproduce very well our experimental findings (Fig. 2a). We confirm the exponentially increasing conductance in the tunnelling regime, $G_{tun}(d) \propto e^{-\beta d}$, for which the distance d between the two electrodes is still large. The slope is independent of the relative alignment of electrode magnetizations, and the computational values of $\beta^{theo} = 1.87$ Å^{-1} (and the work function $W^{theo} = 3.24$ eV) are in agreement with experiment ($\beta = 1.9 \pm 0.3$ Å^{-1}; $W = 3.2$ eV).

Once contact between the tip and the molecule has been established, the variation of $G_{cont}(d)$ with the contact distance d is very weak, just as observed in the experiment. It is, however, still sensitive to the relative orientation of the magnetization of the electrodes. We find that $G_{AP}(d)$ is always much lower than $G_P(d)$. To quantitatively compare with experiment, we consider the theoretical GMR ratio at the distance d at which the ratio $r = G_{tun}/G_{cont}$ matches the value $r \approx 4$ found experimentally. We thus find that GMR ≈ 65% and is only weakly dependent on d.

We now discuss the basic conduction mechanism that underscores the large GMR measured. Pc molecules are characterized by the energetically isolated highest occupied molecular orbital (HOMO) and the nearly doubly degenerate lowest unoccupied molecular orbital (LUMO)[43,44]. We note that the HOMO* levels corresponding to the aromatic group hybridize only very weakly, with almost no amplitude on the bridging nitrogen $(N_b)_4$. In contrast, the LUMO states are located on two of the four aromatic groups, with a strong hybridization to all nitrogen atoms forming the inner macrocycle (see Supplementary Information). Because the nitrogen bond to cobalt includes states at the Fermi energy E_F, (refs 21,45), transport should occur via the (quasi-degenerate) LUMO level. We confirm this fact by examining in Fig. 4a the transmission probability per spin direction $T_{\uparrow,\downarrow}(E)$ near the Fermi energy across a parallel oriented junction. We find that, for both spin

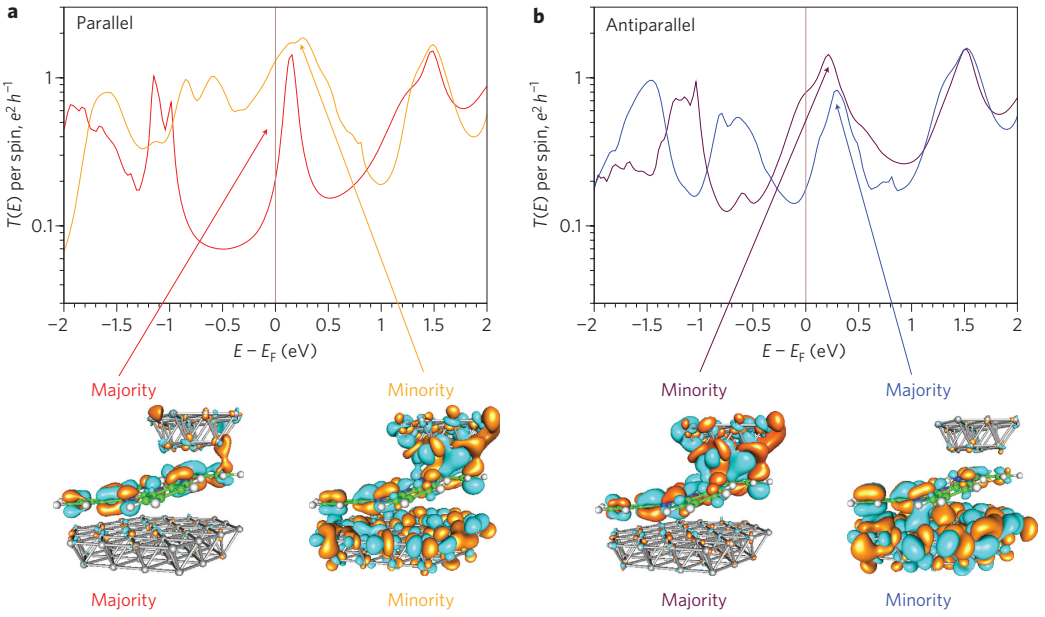

Figure 4 | Molecular orbitals and transmission curves reveal the spin-selective LUMO broadening and the impact on GMR across the H_2Pc molecule. **a**, Transmission probability $T(E)$ of an electron with energy E through a parallel oriented molecular junction for the majority (red) and minority (orange) spin channels and the current-carrying (LUMO) orbitals of the molecular junction at the Fermi energy. Hybridization of the LUMO orbitals with the cobalt states is weak in the majority channel and strong in the minority channel. **b**, Corresponding data for an antiparallel oriented junction. Majority spin electrons are injected from the cobalt surface to the minority spin band of the cobalt tip (violet), and minority spin electrons are injected from the cobalt surface to the majority spin band of the cobalt tip (blue). In this configuration, the LUMO orbitals are hybridized in an asymmetric way between the cobalt surface and the tip, thus accounting for the conductance decrease relative to that found for parallel oriented junctions.

channels, G_P near E_F is indeed dominated by a peak centred slightly above E_F indicating transmission through the LUMO level. We find a similar origin of electron transport for an antiparallel oriented junction (Fig. 4b).

The peak width is determined by the amount of hybridization of the molecular LUMO orbital (through N–Co binding) with the states of the cobalt electrodes. Because the surface density of states of the cobalt electrodes at E_F is enhanced for minority spin electrons as compared to majority spin electrons, the LUMO broadening found for a parallel oriented junction is stronger in the minority transport channel than in the majority channel (Fig. 4a). This broadening asymmetry is, of course, less pronounced for an antiparallel oriented junction (Fig. 4b). Note that our experiments operate at low voltage, 10 meV, in the regime where the current response to the bias voltage is still linear. In this regime, the conductance resembles transmission at the Fermi energy.

The dependence of LUMO broadening on a given spin channel and the relative alignment of electrode magnetizations both, in turn, have a direct impact on the GMR obtained across the molecular junction. Indeed, the conductance across a single level of the quasi-degenerate LUMO generically takes on the Breit–Wigner form[46] (here a factor of 2 accounts for the degeneracy of the LUMO: $G \approx 2\Gamma^{substrate}\Gamma^{tip}/((E_{LUMO}-E_F)^2+(\Gamma^{substrate}+\Gamma^{tip})^2/4)$. This expression considers the energy separation between the LUMO and E_F, as well as the LUMO broadenings (inverse lifetimes) $\Gamma^{substrate}$ and Γ^{tip} due to hybridization to the substrate and tip, respectively. Each is, in turn, split into $\Gamma^{min(maj)}$ depending on the spin channel considered. Because transport is off-resonant, that is, $|E_{LUMO}-E_F| \gg \Gamma^{min,maj}$, we have $G_P \approx 2\ (\Gamma^{min}\Gamma^{min}+\Gamma^{maj}\Gamma^{maj})/(E_{LUMO}-E_F)^2$, while $G_{AP} \approx 4\Gamma^{min}\Gamma^{maj}/(E_{LUMO}-E_F)^2$. Introducing the ratio $\varrho = \Gamma^{maj}/\Gamma^{min}$, we thus find

$$GMR \approx \frac{(\Gamma^{min}-\Gamma^{maj})^2}{2\Gamma^{min}\Gamma^{maj}} = \frac{(1-\varrho)^2}{2\varrho}$$

This simple formula implies two important rules of thumb for spin-polarized transport off-resonance across a molecule. First, the GMR is insensitive to the precise location of the resonance energy provided that E_F lies reasonably within the level broadening. Second, the GMR is mainly indicative of the ratio ϱ of minority and majority molecular orbital broadenings due to hybridization. As such, the GMR may reach larger (here order-of-magnitude) values than its TMR counterpart without molecules.

Several papers have recently described means of tuning this spin-polarized broadening of molecular orbitals near E_F, and the resulting amplitude/sign of interfacial spin polarization useful for spin injection into organic materials. For instance, Barraud and co-workers invoke disorder to explain, within a phenomenological model, the presence at E_F of a localized molecular state that promotes spin-polarized resonant transport in the tunnelling regime[8]. Other reports have considered the impact of intrinsic molecular states near E_F (ref. 22) on spin polarization[21,36,45]. Relative to these reports, our results explicitly reveal the fundamental and applied interest in the direct coupling of two such ferromagnet–molecule interfaces. In this case, the spin selective broadening of the LUMO leads to a highly conductive situation in the parallel configuration with electronic states delocalized across the whole junction, much like the classical and metallic GMR junctions[3,4]. The resulting single-molecule spintronic junction, operating in the contact regime, combines a low resistance (52 kΩ) for high-frequency applications, a low resistance–area product (70 μΩμm^2) for increased density, and a large spintronic response (60%) for enhanced data-processing capabilities. This effect should also be present in nanoscale solid-state devices consisting of two ferromagnetic electrodes separated by a monolayer of organic molecules useful for applications.

Methods

The Cu(111) crystal was cleaned by several cycles of Ar^+ sputtering and annealing. The molecules were evaporated *in situ* from a Knutsen cell heated to ~500 K.

During the deposition process the sample was maintained at 270 K to reduce thermal diffusion of the deposited molecules. dI/dV curves were measured on the bare islands with a lock-in technique.

DFT-based transport calculations were carried out with a homemade code building upon the NEGF formalism and the TURBOMOLE package[41]. Our implementation enabled us to perform transport simulations with free boundary conditions, which for the present case were extended to account for the spin-polarized electronic structure of the magnetic electrodes (for further details, see Supplementary Information). The gradient-corrected approximation (GGA) DFT energy was amended by empirical corrections[47] to account for dispersive van der Waals interactions between the molecule and the surface.

Received 22 November 2010; accepted 14 January 2011; published online 20 February 2011

References

1. Wolf, S. A. *et al.* Spintronics: a spin-based electronics vision for the future. *Science* **294,** 1488–1495 (2001).
2. Zutic, I., Fabian, J. & Sarma, S. D. Spintronics: fundamentals and applications. *Rev. Mod. Phys.* **76,** 323–410 (2004).
3. Baibich, M. N. *et al.* Giant magnetoresistance of (001)Fe/(001)Cr magnetic superlattices. *Phys. Rev. Lett.* **61,** 2472–2475 (1988).
4. Binasch, G., Grünberg, P., Saurenbach, F. & Zinn, W. Enhanced magnetoresistance in layered magnetic structures with antiferromagnetic interlayer exchange. *Phys. Rev. B* **39,** 4828–4830 (1989).
5. Julliere, M. Tunneling between ferromagnetic films. *Phys. Lett.* **54A,** 225–226 (1975).
6. Moodera, J., Kinder, I., Wong, T. & Meservey, R. Large magnetoresistance at room temperature in ferromagnetic thin film tunnel junctions. *Phys. Rev. Lett.* **74,** 3273–3276 (1995).
7. Xiong, Z., Wu, D., Vardeny, Z. & Shi, J. Giant magnetoresistance in organic spin-valves. *Nature* **427,** 821–824 (2004).
8. Barraud, C. *et al.* Unravelling the role of the interface for spin injection into organic semiconductors. *Nature Phys.* **6,** 615–620 (2010).
9. Pople, J. A. & Walmsley, S. H. Bond alternation defects in long polyene molecules. *Mol. Phys.* **5,** 15–20 (1962).
10. Boukari, S. *et al.* Electrical transport across a structurally ordered phthalocyanine film: role of defect states. *Phys. Rev. B* **76,** 033302 (2007).
11. Bowen, M. *et al.* Using half-metallic manganite interfaces to reveal insights into spintronics. *J. Phys. Condens. Matter* **19,** 315208 (2007).
12. Greullet, F. *et al.* Evidence of a symmetry-dependent metallic barrier in fully epitaxial MgO based magnetic tunnel junctions. *Phys. Rev. Lett.* **99,** 187202 (2007).
13. Santos, T. *et al.* Room temperature tunnel magnetoresistance and spin polarized tunneling studies with organic semiconductor barrier. *Phys. Rev. Lett.* **98,** 016601 (2007).
14. Szulczewski, G., Tokuc, H., Oguz, K. & Coey, J. M. D. Magnetoresistance in magnetic tunnel junctions with an organic barrier and an MgO spin filter. *Appl. Phys. Lett.* **95,** 202506 (2009).
15. Nagamine, Y. *et al.* Ultralow resistance–area product of 0.4 Ω $(\mu m)^2$ and high magnetoresistance above 50% in CoFeB/MgO/CoFeB magnetic tunnel junction. *Appl. Phys. Lett.* **89,** 162507 (2006).
16. Fukuzawa, H., Yuasa, H., Hashimoto, S., Iwasaki, H. & Tanaka, Y. Large magnetoresistance ratio of 10% by $Fe_{50}Co_{50}$ layers for current-confined path current-perpendicular-to-plane giant magnetoresistance spin-valve films. *Appl. Phys. Lett.* **87,** 082507 (2005).
17. Elbing, M. *et al.* A single molecule diode. *Proc. Natl Acad. Sci. USA* **102,** 8815–8820 (2005).
18. Park, J. *et al.* Coulomb blockade and the Kondo effect in single-atom transistors. *Nature* **417,** 722–725 (2002).
19. Osorio, E. A., Bjørnholm, T., Lehn, J.-M., Ruben, M. & van der Zant, H. S. J. Single-molecule transport in three-terminal devices. *J. Phys. Condens. Matter* **20,** 374121 (2008).
20. Yu, L. H. *et al.* Kondo resonances and anomalous gate dependence in the electrical conductivity of single-molecule transistors. *Phys. Rev. Lett.* **95,** 256803 (2005).
21. Javaid, S. *et al.* Impact on interface spin polarization of molecular bonding to metallic surfaces. *Phys. Rev. Lett.* **105,** 077201 (2010).
22. Takács, A. F. *et al.* Electron transport through single phthalocyanine molecules studied using scanning tunneling microscopy. *Phys. Rev. B* **78,** 233404 (2008).
23. Wende, H. *et al.* Substrate-induced magnetic ordering and switching of iron porphyrin molecules. *Nat. Mater.* **6,** 516–520 (2007).
24. Iacovita, C. *et al.* Visualizing the spin of individual cobalt–phthalocyanine molecules. *Phys. Rev. Lett.* **101,** 116602 (2009).
25. Joachim, C., Gimzewski, J. K., Schlittler, R. R. & Chavy, C. Electronic transparence of a single C_{60} molecule. *Phys. Rev. Lett.* **74,** 2102–2105 (1995).
26. Haiss, W. *et al.* Precision control of single-molecule electrical junctions. *Nat. Mater.* **5,** 995–1002 (2006).
27. Néel, N. *et al.* Controlled contact to a C_{60} molecule. *Phys. Rev. Lett.* **98,** 065502 (2007).
28. Venkataraman, L. *et al.* Single-molecule circuits with well-defined molecular conductance. *Nano Lett.* **6,** 458–462 (2006).
29. Li, Z. *et al.* Conductance of redox-active single molecular junctions: an electrochemical approach. *Nanotechnology* **18,** 044018 (2007).
30. Balashov, T., Takács, A. F., Wulfhekel, W. & Kirschner, J. Magnon excitation with spin-polarized scanning tunneling microscopy. *Phys. Rev. Lett.* **97,** 187201 (2006).
31. Kuch, W. *et al.* Magnetic dichroism study of the valence-band structure of perpendicularly magnetized Co/Cu(111). *Phys. Rev. B* **57,** 5340–5346 (1998).
32. Pietzsch, O., Kubetzka, A., Bode, M. & Wiesendanger, R. Spin-polarized scanning tunneling spectroscopy of nanoscale cobalt islands on Cu(111). *Phys. Rev. Lett.* **92,** 057202 (2004).
33. Tersoff, J. & Hamann, D. R. Theory of the scanning tunneling microscope. *Phys. Rev. B* **31,** 805–813 (1985).
34. Diekhöner, L. *et al.* Surface states of cobalt nanoislands on Cu(111). *Phys. Rev. Lett.* **90,** 236801 (2003).
35. Lippel, P. H., Wilson, R. J., Miller, M. D., Wöll, C. & Chiang, S. High-resolution imaging of copper–phthalocyanine by scanning-tunneling microscopy. *Phys. Rev. Lett.* **62,** 171–174 (1989).
36. Atodiresei, N. *et al.* Design of the local spin polarization at the organic-ferromagnetic interface. *Phys. Rev. Lett.* **105,** 066601 (2010).
37. Moresco, F. Manipulation of large molecules by low-temperature STM: model systems for molecular electronics. *Phys. Rep.* **399,** 175–225 (2004).
38. Temirov, R., Lassise, A., Anders, F. B. & Tautz, F. S. Kondo effect by controlled cleavage of a single-molecule contact. *Nanotechnology* **19,** 065401 (2008).
39. Joachim, C., Gimzewski, J. K., Schlittler, R. R. & Chavy, C. Electronic transparence of a single C_{60} molecule. *Phys. Rev. Lett.* **74,** 2102–2105 (1995).
40. Oka, H. *et al.* Spin-dependent quantum interference within a single magnetic nanostructure. *Science* **327,** 843–846 (2010).
41. Arnold, A., Weigend, F. & Evers, F. Quantum chemistry calculations for molecules coupled to reservoirs: formalism, implementation and application to benzene–dithiol. *J. Chem. Phys.* **126,** 174101 (2007).
42. Heinrich, B. W. *et al.* Direct observation of the tunnelling channels of a chemisorbed molecule. *Phys. Chem. Lett.* **1,** 1517–1523 (2010).
43. Rosa, A. & Baerends, E. J. Origin and relevance of the staggering in one-dimensional molecular metals. A density functional study of metallophthalocyanine model dimers. *Inorg. Chem.* **31,** 4717–4726 (1992).
44. Rosa, A., Ricciardi, G., Baerends, E. J. & van Gisbergen S. J. A. The optical spectra of NiP, NiPz, NiTBP, and NiPc: electronic effects of meso-tetraaza substitution and tetrabenzo annulation. *J. Phys. Chem. A* **105,** 3311–3327 (2001).
45. Brede, J. *et al.* Spin- and energy-dependent tunneling through a single molecule with intramolecular spatial resolution. *Phys. Rev. Lett.* **105,** 047204 (2010).
46. Breit, G. & Wigner, E. Capture of slow neutrons. *Phys. Rev. B* **49,** 519–531 (1936).
47. Grimme, S. Semiempirical GGA-type density functional constructed with a long-range dispersion correction. *J. Comp. Chem.* **27,** 1787–1799 (2006).

Acknowledgements

The authors thank O. Hampe, J. Kortus, K. Fink, S. Boukari, Xi Chen, M. Alouani, R. Mattana, J. van Ruitenbeek and P. Seneor for useful communications. The authors also acknowledge support from the Deutsche Forschungsgemeinschaft (WU 349/3-1 and SPP1243), the Center for Functional Nanostructures, the French–German University, the Alexander von Humboldt foundation, and the Agence Nationale de la Recherche (ANR-06-NANO-033-01) as well as from the Yamada Science Foundation and the Asahi Glass Foundation.

Author contributions

S.S. and W.W. conceived and designed the experiments. S.S., Y.N., T.K.Y. and An.B. performed the experiments. S.S., Y.N. and An.B. analysed the data. Al.B. and F.E. designed and performed the calculations. M.B. and E.B. provided purified molecules. S.S., Al.B., T.K.Y., F.E., M.B., E.B. and W.W. co-wrote the paper. All authors discussed the results and commented on the manuscript.

Additional information

The authors declare no competing financial interests. Supplementary information accompanies this paper at www.nature.com/naturenanotechnology. Reprints and permission information is available online at http://npg.nature.com/reprintsandpermissions/. Correspondence and requests for materials should be addressed to W.W.